Heterogeneous Catalysis

DOI: 10.1002/anie.201006014

Highly Active Catalysts of Gold Nanoparticles Supported on Three-Dimensionally Ordered Macroporous $LaFeO_3$ for Soot Oxidation**

Yuechang Wei, Jian Liu, Zhen Zhao,* Yongsheng Chen, Chunming Xu, Aijun Duan, Guiyuan Jiang, and Hong He*

Heterogeneous catalytic reactions containing solid particles as reactant are an important and complex class of chemical reactions. The contact area between the catalyst and solid reactant is of great importance in heterogeneous catalysis. The soot emitted from diesel engines as a typical solid particle[1] has caused acute health problems to human beings. Efficient exhaust gas treatment systems are dependent on the catalytic performance of oxidation catalysts, especially catalysts with very low ignition temperature (T_{ig}). Some nonnoble metal oxide catalysts such as transition-metal oxides,[2] alkaline metal oxides,[3] perovskite-like type oxides,[4] and ceria-based oxides[5] have exhibited good catalytic performance for diesel soot combustion. However, it is very hard to get the T_{ig} lower than 250°C (as seen by Table S1 in the Supporting Information). So far, noble-metal catalysts are still the best catalytic system for soot combustion, for example, Pt/SiO_2 has the lowest T_{ig} value (247°C),[6] and only Pt-based catalysts are currently commercialized under practical conditions despite its expensive price.[7] Generally, soot particles whose sizes ranging from 20 nm to 1 μm have difficulty entering the inner pores of general catalysts, which may influence the contact area between soot and catalyst. Three-dimensionally ordered macroporous (3DOM)[8] materials with big pore size (> 50 nm) can permit solid reactant to enter the inner pores and to easily transport and diffuse. Therefore, the tangible active points between reactant and catalyst will be increased dramatically. Recently, 3DOM oxides show good catalytic activity for diesel soot oxidation,[9] but their catalytic performance at low temperature is limited by the intrinsic activity of material. Since the pioneering studies by Haruta et al.,[10] supported gold catalysts have received much attention owing to their unusual and somewhat unexpected catalytic properties for oxidation reactions.[11] It is commonly accepted that the size dependence of Au particles is the most intriguing issue for oxidation catalysis,[12] because the chemisorption and activation of O_2 depends on Au particle size.[13] Thus, 3DOM oxide-supported gold catalysts, which combine the advantages of good contact between soot and catalyst by 3DOM supports and the highly active sites for activation of O_2 by gold clusters with suitable nanosize, should exhibit super catalytic performance and be promising to substitute Pt-based catalyst for soot oxidation.

Effective control of the dispersion and size of supported gold particles is a primary goal of catalyst design and is quite challenging. Generally, nucleation and growth of metal nanocrystals govern the particle size and morphology of the nanoparticles in the synthesis process by coprecipitation or reduction.[14] Kinetic control of the nucleation and growth process may be an operative means to regulate the size of nanocrystals, for example, through a highly homogeneous dispersion of reductant and the addition of an organic stability reagent into precursor solution. Herein, we synthesized a series of 3DOM $Au_n/LaFeO_3$ catalysts by the new gas-bubbling-assisted membrane reduction (GBMR) method. The fabrication of gold nanoparticles on the surface of 3DOM $LaFeO_3$ support is shown in Scheme 1. Firstly, $AuCl_4^-$ ions are adsorbed and anchored on surface OH_2^+ groups on the $LaFeO_3$ support formed because of the pH value of the solution (pH 5) is lower than the isoelectric point of the $LaFeO_3$ support. Simultaneously, a hybrid between $AuCl_4^-$ ions and capping ligands of the poly(*N*-vinyl-2-pyrrolidone)

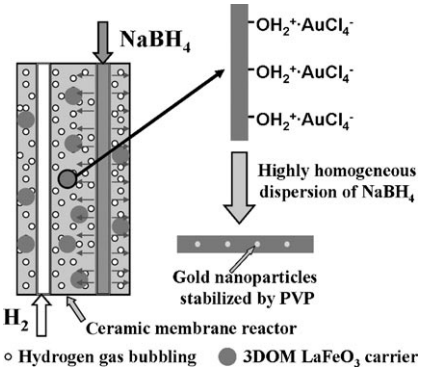

Scheme 1. Preparation of gold nanoparticles on the surface of 3DOM $LaFeO_3$ carrier by GBMR method.

[*] Y. Wei, Dr. J. Liu, Prof. Z. Zhao, Prof. C. Xu, Dr. A. Duan, Dr. G. Jiang
State Key Laboratory of Heavy Oil Processing
China University of Petroleum
18#, Fuxue Road, Chang Ping, Beijing 102249 (China)
Fax: (+86) 10-6972-4721
E-mail: liujian@cup.edu.cn
zhenzhao@cup.edu.cn
Prof. Y. Chen
EMS Energy Institute and Department of Energy and Mineral Engineering
The Pennsylvania State University
University Park, PA 16802 (USA)
Prof. H. He
College of Environmental and Energy Engineering
Beijing University of Technology
Beijing 100124 (China)

[**] This work was financially supported by the NSFC (20833011, 20803093), 863 Program (2009AA06Z313), and CNPC Innovation Fund (2010D-5006-0402).

Supporting information for this article is available on the WWW under http://dx.doi.org/10.1002/anie.201006014.

(PVP) might form. When $NaBH_4$ was highly homogeneously dispersed into the holes ($d = 40$ nm) of the ceramic membrane tubular reactor, the reduction of $AuCl_4^-$ occurred immediately to give Au nucleus with convenient protection, resulting in restriction of the growth of crystal nucleus on the surface of 3DOM $LaFeO_3$ supports. The steady H_2 gas bubbling promotes mass transfer, reduces dead space, and improves the uniform distribution of Au nanoparticles on the 3DOM $LaFeO_3$ carrier. The appropriate adjustment of reaction conditions, including the PVP concentration and the hole size of ceramic membrane, provides an effective way to control the dispersion and size of Au nanoparticles. The actual content of Au in catalysts was determined by inductively coupled plasma atomic emission spectrometry (ICP-AES) (Table S3 in the Supporting Information).

Figure 1 shows SEM and TEM images, as well as the size distribution of Au nanoparticles of 3DOM $Au_{0.04}/LaFeO_3$ catalysts obtained by GBMR method. The SEM image exhibits macroporous structure containing periodic voids

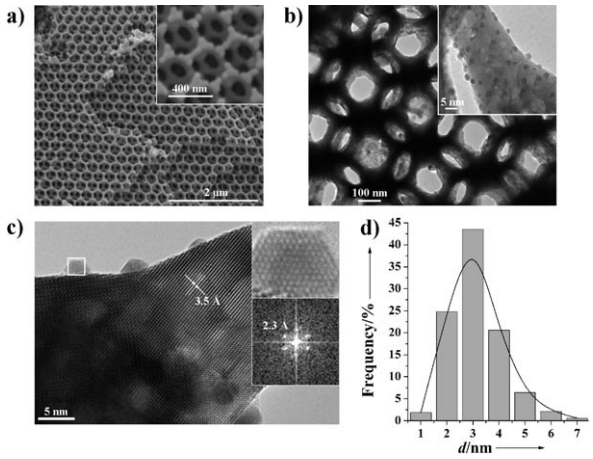

Figure 1. a) SEM, b) TEM, and c) HRTEM images and d) size distribution of Au nanoparticles of 3DOM $Au_{0.04}/LaFeO_3$. The insets in (a) and (b) show an enlarged area, and the inset in (c) shows an enlarged Au particle whose lattice fringes correspond to the fcc (111) plane at 2.3 Å in a fast Fourier transform (FFT) image.

with average diameter of 250 nm, and the next layer is highly visible in the inset image (Figure 1 a). The voids are interconnected through open windows, approximately 100 nm in diameter, which is a similar well-defined 3DOM structure to $LaFeO_3$ supports (Figure S1). The 3DOM structure with overlapped pores can be clearly observed in the TEM image in Figure 1 b, and supported Au nanoparticles precipitated on the surface of 3DOM $LaFeO_3$ support can be also clearly observed in the inset image (Figure 1 b); all Au particles are highly dispersed and uniform in size. The HRTEM image of $Au_{0.04}/LaFeO_3$ in Figure 1 c demonstrates that the clear lattice fringes with spacing of 3.5 Å corresponding to the (111) plane of orthorhombic phased $LaFeO_3$ confirmed by XRD measurement (Figure S9) and FTIR spectra (Figure S10).[15] Magnification of the Au particles in the inset image of Figure 1 c shows that the hemispherical gold particles located on the surface of the $LaFeO_3$ carrier are crystalline, expose the fcc (111) plane, and have a contact angle of about 90°. It is evident that the roughness originates from the contact between the Au nanoparticles and the $LaFeO_3$ support, which is an indication of the existence of a strong metal–support interaction. The Au particle size is in the range of 1–7 nm with a narrow distribution (Figure 1 d) and a mean diameter of 3.0 nm by statistic analysis of more than 300 Au particles (Table S3).

The catalytic activity of the materials for soot oxidation was evaluated by temperature-programmed oxidation (TPO) method, and the results are listed in Table 1. Among the TPO results, 3DOM $LaFeO_3$ catalyst has higher catalytic activity than the corresponding particle catalysts, indicating that the open and interconnected macropores give more facilities for the contact between soot and catalysts. The catalytic activities, as well as the T_{ig} and S_{CO_2} values, for soot oxidation were remarkably enhanced by the Au nanoparticles supported on the surface of 3DOM $LaFeO_3$ supports. Increasing the gold loading ($n < 0.04$) enhanced the catalytic activity of 3DOM $Au_n/LaFeO_3$ catalysts owing to the increased number of active site of supported Au nanoparticles. However, the limitation of contact area between soot and active site is a key factor for solid (reactant)–solid (catalyst) reactions. The actual contact area between soot and catalyst will not increase with the increasing of Au content in the catalyst ($n = 0.04$–0.08). Therefore, the catalytic activities (T_{ig}) of 3DOM $Au_n/LaFeO_3$ ($n = 0.04$, 0.06, 0.08) are similar. 3DOM $Au_{0.04}/LaFeO_3$ with Au particle size of 3.0 nm exhibited highly catalytic activity, (T_{ig}, T_m, and $S^m_{CO_2}$ are 228, 368 °C, and 99.7 %, respectively). As far as we know, this T_{ig} value is the lowest reported (including Pt-based catalysts, simple oxides, or compound oxides)[3–8] for soot oxidation under the condition of the loose contact between catalyst and soot. The very high S_{CO_2} results (Figure S15) are attributed to supported Au catalyst, which has super catalytic performance for CO oxidation. Our experimental results (Figure S12–14) also indicate that the catalytic performances of supported Au catalysts at low temperature (< 250 °C) is dependent on the Au particle sizes, which would affect the adsorption and activation of oxygen on Au (111).[16] However, at relatively high temperature (> 250 °C), the catalytic activity is strongly

Table 1: Temperatures and selectivity to CO_2 of soot combustion over catalysts and without catalyst (loose contact).[a]

Catalyst	T_{ig} [°C]	T_m [°C]	$S^m_{CO_2}$ [%]
pure soot	482	585	55.0
$LaFeO_3$ (particles)	378	486	80.0
$LaFeO_3$ (3DOM)	347	415	92.2
$Au_{0.005}/LaFeO_3$ (4.2 nm)	282	379	99.1
$Au_{0.01}/LaFeO_3$ (4.0 nm)	277	371	99.5
$Au_{0.02}/LaFeO_3$ (3.7 nm)	264	369	99.6
$Au_{0.04}/LaFeO_3$ (3.0 nm)	228	368	99.7
$Au_{0.06}/LaFeO_3$ (2.9 nm)	230	366	99.6
$Au_{0.08}/LaFeO_3$ (2.8 nm)	229	359	99.7
$Au_{0.04}/LaFeO_3$ (5.3 nm)	271	380	99.7
$Au_{0.04}/LaFeO_3$ (7.8 nm)	285	384	99.6
Pt/SiO_2[b]	247	312	99.5

[a] Conditions: 5 % O_2 and 0.2 % NO in Ar, 50 mL min^{-1}; the mass ratio (catalyst/soot) is 10:1. [b] Ref. [6a].

dependent on the NO gas, because NO_2 derived from NO oxidized is used as intermediate to catalyze the soot oxidation.[4a,6a,b,7c,e] Technical developments of diesel engines strive to suppress raw NO_x emissions, which call for a catalyst system that accelerates soot oxidation in the absence of NO_x. Because of the formation of active oxygen species over Au surface, the catalytic performances of supported Au catalysts at low temperature are still very good in absence of NO; the T_{ig} value over $Au_{0.04}/LaFeO_3$ catalyst is 231 °C (Figure S14). To clearly observe the effect of thermal pretreatment on the size of supported Au nanoparticles, 3DOM $Au_{0.04}/LaFeO_3$ (3.0) catalyst was calcined at 550 °C for 4 h in static air. The average size of Au nanoparticles (8.2 nm) becomes larger (Figure S16). The catalytic activity (T_{ig} = 287 °C) of 3DOM $Au_{0.04}/LaFeO_3$ (8.2 nm) catalyst remarkably decreased (Figure S17). The result indicates again that the catalytic activity of 3DOM $Au_n/LaFeO_3$ catalysts at low temperature is dependent on the Au particle sizes. The effect of the water and SO_2 were also investigated (Figure S18). The catalytic activities of 3DOM $Au_{0.04}/LaFeO_3$ (3.0 nm) catalyst for soot combustion are relatively unchanged, indicating that the catalyst has good resistance to water and sulfur.

Generally speaking, the catalytic performance of materials for oxidation reaction is correlated with the capability to activate oxygen. As shown in Figure 2a, O_2 temperature-programmed desorption (O_2-TPD) results indicated that the O_2 desorption peak of pure $LaFeO_3$ carrier is very weak. However, the O_2-TPD profile of 3DOM $Au_{0.04}/LaFeO_3$ (3.0 nm) catalyst shows that there are four oxygen desorption peaks at 70, 183, 385, and 700 °C, which are assigned to the desorption of physical adsorption oxygen species (O_2), chemisorbed surface-active oxygen species (O_2^-, O^-), and lattice oxygen (O^{2-}), respectively.[17] It is clear that the amount of active surface oxygen species of the catalyst increases with increasing gold content (Table S4). As shown in Figure 2b, the intensity of oxygen desorption peaks decreases remarkably with increasing Au particle size, indicating that the adsorption and activation of oxygen is dependent on the effective size of supported Au particles, and the catalytic performance is correlated with the amount of active surface oxygen species (Table S4 and Figure S19). This result is accorded with the interpretation for the Au particle size-effect by Goodman and co-workers.[18] When the Au particle size is 3 nm, the electron-donating property of Au particle is strong, which results in much higher ability to activate and dissociate molecular oxygen.

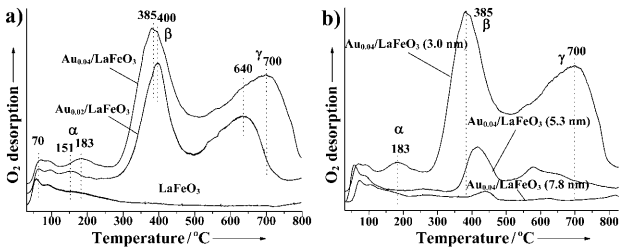

Figure 2. O_2-TPD curves of 3DOM $Au_n/LaFeO_3$ catalysts with different Au loading contents (a) and particle sizes (b).

To further examine the electronic properties of the supported Au nanoparticles and absorbed oxygen, 3DOM $Au_{0.04}/LaFeO_3$ catalysts with different Au particles sizes were studied by XPS (Figure 3). It was found that Au^0 and Au^+ are

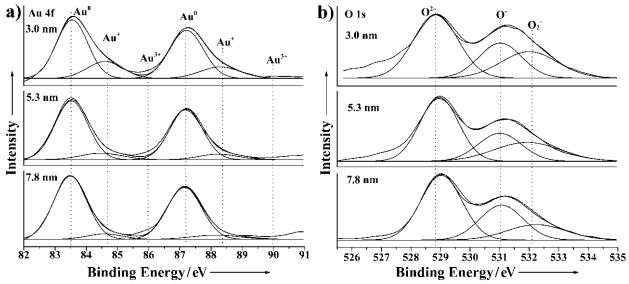

Figure 3. XPS spectra of a) Au 4f and b) O 1s peaks of the 3DOM $Au_{0.04}/LaFeO_3$ catalysts with different Au particle sizes.

the main species on the surface of catalysts, and increasing the Au particle size significantly decreases the content of Au^+ in the catalysts owing to transformation of gold clusters from Au^+ oxide to Au^0 metal. The increasing Au particle size is associated with a decrease in the d-electron density of the Au atoms and the onset of reactivity to oxygen in air,[19] which is in accordance with the amount of surface active oxygen species (O_2^-, O^-) decreasing in Figure 3b and Table S5. The results correspond with the change of O_2 desorption peak in O_2-TPD curves, indicating that Au particle size is a critical factor in the adsorption and activation of oxygen,[20] and the size-dependent alteration of electronic structure gives rise to unusual catalytic properties.

In summary, 3DOM $Au_n/LaFeO_3$ catalysts with controlled Au particle sizes were synthesized by a novel GBMR method. 3DOM $Au_n/LaFeO_3$ catalysts show super catalytic activity for soot oxidation, especially at low temperatures, which is attributed to the activation of oxygen on Au particles with appropriate size. Although only the catalyst of 3DOM $LaFeO_3$-supported Au particles was used as a case study, we believe that this method can be extended to other circumstances with other active metals, supports, and coatings. The samples with 3DOM structure supports and nanoparticle active sites may be useful for fundamental research on metal–support synergetic effect and potential practical applications in the catalytic oxidation of solid particles if the thermal stability of Au-based catalysts can be further improved.

Experimental Section

The synthesis of monodispersed PMMA microsphere, the assembly template, and preparation of 3DOM $LaFeO_3$ perovskite-type complex oxides supports by the colloidal crystal template method are similar to that described previously.[3] Detailed procedures are described in the Supporting Information.

The synthesis of 3DOM $Au_n/LaFeO_3$ catalysts was carried out by the GBMR method developed in our lab. A schematic diagram of the new method is presented in the Supporting Information in Scheme S2, and reagent specifications are shown in Table S2. A typical preparative procedure is described as follows: The PVP solution as a stabilizer and 3DOM $LaFeO_3$ support were added into

$HAuCl_4$ solution. The mixture solution was driven by a peristaltic pump to form a cycling flow. A reductant solution ($NaBH_4$) was injected into the membrane rector with two ceramic membrane tubes by a constant flow pump. Meanwhile, hydrogen gas was also injected into the membrane rector. The $NaBH_4$ solution was infiltrated through the abundant holes ($d = 40$ nm) on the wall of the ceramic tubes into the glass tube reactor, where the reduction of metal ions occurred immediately when the two solutions met. The hydrogen bubbling-assisted stirring operation (40 mL min^{-1}) was developed to vigorously stir the solution and to make the reaction homogeneous. The synthesis process was stopped after complete consumption of the $NaBH_4$ solution. Then, the product was filtered and washed until Cl^- was completely removed according to a test with $AgNO_3$, and the final products were dried in an oven at 100 °C to obtain the desired 3DOM $Au_n/LaFeO_3$ catalysts.

The catalytic performances of the catalysts were evaluated with a temperature-programmed oxidation reaction (TPO) on a fixed-bed tubular quartz system ($\phi = 8$ mm), and each TPO run from 150 to 650 °C at a 2 °C min^{-1} rate. The soot was Printex-U (diameter, 25 nm, purchased from Degussa). The catalyst (100 mg) and soot (10 mg) were mixed with a spatula to reproduce the loose contact mode. Reactant gases (50 mL min^{-1}) contain 5 % O_2 and 0.2 % NO balanced with Ar. The outlet gas compositions were analyzed with an online gas chromatograph (GC, Sp-3420, Beijing) by using FID detectors. The selectivity to CO_2 formation (S_{CO_2}) was defined as the CO_2 concentration (C_{CO_2}) divided by the sum of the CO_2 and CO outlet concentration, that is, $S_{CO_2} = C_{CO_2}/(C_{CO} + C_{CO_2})$. The catalytic activity was evaluated by the values of T_{ig} and T_m. T_{ig} was defined as the temperature at which 10 % of the soot was oxidized, and T_m was the peak temperature at which the maximum C_{CO_2} value was obtained during the TPO procedure. In all TPO experiments, the reaction was not finished until the soot was completely burnt off.

Received: September 25, 2010
Published online: February 3, 2011

Keywords: gold · heterogeneous catalysis · nanoparticles · O–O activation

[1] a) K. Villani, C. E. A. Kirschhock, D. Liang, G. V. Tendeloo, J. A. Martens, *Angew. Chem.* **2006**, *118*, 3178; *Angew. Chem. Int. Ed.* **2006**, *45*, 3106; b) R. Kimura, J. Wakabayashi, S. P. Elangovan, M. Ogura, T. Okubo, *J. Am. Chem. Soc.* **2008**, *130*, 12844.

[2] a) D. Reichert, T. Finke, N. Atanassova, H. Bockhorn, S. Kureti, *Appl. Catal. B* **2008**, *84*, 803; b) F. E. López-Suárez, A. Bueno-López, M. J. Illán-Gómez, *Appl. Catal. B* **2008**, *84*, 651; c) J. Liu, Z. Zhao, C. Xu, A. Duan, G. Jiang, *J. Phys. Chem. C* **2008**, *112*, 5930.

[3] a) N. E. Olong, K. Stöwe, W. F. Maier, *Appl. Catal. B* **2007**, *74*, 19; b) S. Mosconi, I. D. Lick, A. Carrascull, M. I. Ponzi, E. N. Ponzi, *Catal. Commun.* **2007**, *8*, 1755; c) B. Białobok, J. Trawczyński, T. Rzadki, W. Miśta, M. Zawadzki, *Catal. Today* **2007**, *119*, 278; d) N. Nejar, M. Makkee, M. J. Illán-Gómez, *Appl. Catal. B* **2007**, *75*, 11; e) D. Fino, E. Cauda, D. Mescia, N. Russo, G. Saracco, V. Specchia, *Catal. Today* **2007**, *119*, 257; g) E. Aneggi, C. Leitenburg, G. Dolcetti, A. Trovarelli, *Catal. Today* **2008**, *136*, 3; f) L. Castoldi, R. Matarrese, L. Lietti, P. Forzatti, *Appl. Catal. B* **2009**, *90*, 278.

[4] a) H. Wang, Z. Zhao, C. Xu, J. Liu, *Catal. Lett.* **2005**, *102*, 251; b) J. Liu, Z. Zhao, C. Xu, A. Duan, *Appl. Catal. B* **2008**, *78*, 61; c) N. Russo, S. Furfori, D. Fino, G. Saracco, V. Specchia, *Appl. Catal. B* **2008**, *83*, 85; d) J. L. Hueso, A. Caballero, M. Ocaña, A. R. González-Elipe, *J. Catal.* **2008**, *257*, 334; e) F. E. López-Suárez, S. Parres-Esclapez, A. Bueno-López, M. J. Illán-Gómez, B. Ura, J. Trawczynski, *Appl. Catal. B* **2009**, *93*, 82.

[5] a) R. Cousin, S. Capelle, E. Abi-Aad, D. Courcot, A. Aboukaïs, *Appl. Catal. B* **2007**, *70*, 247; b) K. Krishna, A. Bueno-López, M. Makkee, J. A. Moulijn, *Appl. Catal. B* **2007**, *75*, 189; c) J. Liu, Z. Zhao, J. Wang, C. Xu, A. Duan, G. Jiang and Q. Yang, *Appl. Catal. B* **2008**, *84*, 185; d) S. B. Simonsen, S. Dahl, E. Johnson, S. Helveg, *J. Catal.* **2008**, *255*, 1; e) I. Atribak, A. Bueno-López, A. García-García, *J. Catal.* **2008**, *259*, 123; I. Atribak, A. Bueno-López, A. García-García, *Appl. Catal. B* **2009**, *92*, 126; f) J. Liu, Z. Zhao, J. Lan, C. Xu, A. Duan, G. Jiang, X. Wang, H. He, *J. Phys. Chem. C* **2009**, *113*, 17114.

[6] a) J. Oi Uchisawa, A. Obuchi, Z. Zhao, S. Kushiyama, *Appl. Catal. B* **1998**, *18*, 183; b) J. Oi Uchisawa, S. Wang, T. Nanba, A. Ohi, A. Obuchi, *Appl. Catal. B* **2003**, *44*, 207.

[7] a) P. Hawker, N. Myers, G. Huthwohl, H. T. Vogel, B. Bates, L. Magnusson, P. Bronnehberg, *SAE Paper* 970182, **1997**; b) C. A. Querini, L. M. Cornaglia, M. A. Ulla, E. E. Miro, *Appl. Catal. B* **1999**, *20*, 165; c) C. Görsmann, *Monatsh. Chem.* **2005**, *136*, 91; d) M. V. Twigg, *Appl. Catal. B* **2007**, *70*, 2.

[8] a) P. D. Yang, T. Deng, D. Y. Zhao, P. Y. Feng, D. Pine, B. F. Chmelka, G. M. Whitesides, G. D. Stucky, *Science* **1998**, *282*, 2244; b) C. Li, L. Qi, *Angew. Chem.* **2008**, *120*, 2422; *Angew. Chem. Int. Ed.* **2008**, *47*, 2388; c) X. Meng, R. Al-Salman, J. Zhao, N. Borissenko, Y. Li, F. Endres, *Angew. Chem.* **2009**, *121*, 2741; *Angew. Chem. Int. Ed.* **2009**, *48*, 2703.

[9] a) G. Zhang, Z. Zhao, J. Liu, G. Jiang, A. Duan, J. Zheng, S. Chen, R. Zhou, *Chem. Commun.* **2010**, *46*, 457; b) J. Xu, J. Liu, Z. Zhao, J. Zheng, G. Zhang, A. Duan, G. Jiang, *Catal. Today* **2010**, *153*, 136.

[10] M. Haruta, T. Kobayashi, H. Sano, N. Yamada, *Chem. Lett.* **1987**, 405.

[11] a) M. C. Daniel, D. Astruc, *Chem. Rev.* **2004**, *104*, 293; b) D. Astruc, F. Lu, R. Aranzaes, *Angew. Chem.* **2005**, *117*, 8062; *Angew. Chem. Int. Ed.* **2005**, *44*, 7852; c) A. Grirrane, A. Corma, H. Garica, *Science* **2008**, *322*, 1661; d) T. Mitsudome, A. Noujima, Y. Mikami, T. Mizugaki, K. Jitsukawa, *Angew. Chem.* **2010**, *122*, 5677; *Angew. Chem. Int. Ed.* **2010**, *49*, 5545.

[12] a) M. S. Chen, D. W. Goodman, *Chem. Soc. Rev.* **2008**, *37*, 1860; b) A. A. Herzing, C. J. Kiely, A. F. Carley, P. Landon, G. J. Hutchings, *Science* **2008**, *321*, 1331; c) Y. Liu, C. Jia, J. Yamasaki, O. Terasaki, F. Schüth, *Angew. Chem.* **2010**, *122*, 5907; *Angew. Chem. Int. Ed.* **2010**, *49*, 5771.

[13] a) Y. D. Kim, M. Fischer, G. Gantefor, *Chem. Phys. Lett.* **2003**, *377*, 170; b) L. M. Molina, B. Hammer, *J. Chem. Phys.* **2005**, *123*, 161104; c) W. Huang, H. J. Zhai, L. S. Wang, *J. Am. Chem. Soc.* **2010**, *132*, 4344.

[14] a) B. L. Cushing, V. L. Kolesnichenko, C. J. O'Conno, *Chem. Rev.* **2004**, *104*, 3893; b) N. Zheng, G. D. Stucky, *J. Am. Chem. Soc.* **2006**, *128*, 14278; c) L. Liu, T. Wei, X. Guan, X. Zi, H. He, H. X. Dai, *J. Phys. Chem. C* **2009**, *113*, 8595; d) K. K. R. Datta, B. V. S. Reddy, K. Ariga, A. Vinu, *Angew. Chem.* **2010**, *122*, 6097; *Angew. Chem. Int. Ed.* **2010**, *49*, 5961.

[15] N. Escalona, S. Fuentealba, G. Pecchi, *Appl. Catal. A* **2010**, *381*, 253.

[16] a) N. Lopez, J. K. Nørskov, *J. Am. Chem. Soc.* **2002**, *124*, 11262; b) N. Weiher, A. M. Beesley, N. Tsapatsaris, L. Delannoy, C. Louis, J. A. van Bokhoven, S. L. M. Schroeder, *J. Am. Chem. Soc.* **2007**, *129*, 2240; c) M. Kotobuki, R. Leppelt, D. A. Hansgen, D. Widmann, R. J. Behn, *J. Catal.* **2009**, *264*, 67.

[17] C. Ma, Z. Mu, J. Li, Y. Jin, J. Cheng, G. Lu, Z. Hao, S. Qiao, *J. Am. Chem. Soc.* **2010**, *132*, 2608.

[18] M. Valden, X. Lai, D. W. Goodman, *Science* **1998**, *281*, 1647.

[19] M. Turner, V. B. Golovko, O. P. H. Vaughan, P. Abdulkin, A. Berenguer-Murcia, M. S. Tikhov, B. F. G. Johnson, R. M. Lambert, *Nature* **2008**, *454*, 981.

[20] N. Yi, R. Si, H. Saltsburg, M. Flytzani-Stephanopoulos, *Energy Environ. Sci.* **2010**, *3*, 831.

